Quadrupole Transition Strength in the ^{74}Ni Nucleus and Core Polarization Effects in the Neutron-Rich Ni Isotopes

T. Marchi,[1,2,*] G. de Angelis,[1] J. J. Valiente-Dobón,[1] V. M. Bader,[3] T. Baugher,[3] D. Bazin,[3] J. Berryman,[3] A. Bonaccorso,[4] R. Clark,[5] L. Coraggio,[6] H. L. Crawford,[5] M. Doncel,[7] E. Farnea,[8] A. Gade,[3] A. Gadea,[9] A. Gargano,[6] T. Glasmacher,[3] A. Gottardo,[1] F. Gramegna,[1] N. Itaco,[10,6] P. R. John,[8,2] R. Kumar,[11] S. M. Lenzi,[8,2] S. Lunardi,[8,2] S. McDaniel,[3] C. Michelagnoli,[8,2] D. Mengoni,[8,2] V. Modamio,[1] D. R. Napoli,[1] B. Quintana,[7] A. Ratkiewicz,[3] F. Recchia,[8,2] E. Sahin,[1] R. Stroberg,[3] D. Weisshaar,[3] K. Wimmer,[3] and R. Winkler[3]

[1]*Istituto Nazionale di Fisica Nucleare, Laboratori Nazionali di Legnaro, 35020 Legnaro, Italy*
[2]*Dipartimento di Fisica e Astronomia dell'Università degli Studi di Padova, 35131 Padova, Italy*
[3]*National Superconducting Cyclotron Laboratory, Michigan State University, East Lansing, Michigan 48824, USA*
[4]*Istituto Nazionale di Fisica Nucleare, Sezione di Pisa, 56127 Pisa, Italy*
[5]*Nuclear Science Division, Lawrence Berkeley National Laboratory, Berkeley, California 94720, USA*
[6]*Istituto Nazionale di Fisica Nucleare, Sezione di Napoli, 80126 Napoli, Italy*
[7]*Laboratorio De Radiaciones Ionizantes, Universidad de Salamanca, 37008 Salamanca, Spain*
[8]*Istituto Nazionale di Fisica Nucleare, Sezione di Padova, 35131 Padova, Italy*
[9]*Instituto de Física Corpuscular, CSIC-Universitat de València, 46980 València, Spain*
[10]*Dipartimento di Fisica, Università di Napoli Federico II, 80126 Napoli, Italy*
[11]*Department of Physics, Deenbandhu Chhoturam University of Science and Technology, Murthal, Sonepat, Haryana 131039, India*

(Received 30 April 2014; published 28 October 2014)

The reduced transition probability $B(E2;0^+ \to 2^+)$ has been measured for the neutron-rich nucleus ^{74}Ni in an intermediate energy Coulomb excitation experiment performed at the National Superconducting Cyclotron Laboratory at Michigan State University. The obtained $B(E2;0^+ \to 2^+) = 642^{+216}_{-226}\ e^2\,\mathrm{fm}^4$ value defines a trend which is unexpectedly small if referred to ^{70}Ni and to a previous indirect determination of the transition strength in ^{74}Ni. This indicates a reduced polarization of the $Z = 28$ core by the valence neutrons. Calculations in the $pfgd$ model space reproduce well the experimental result indicating that the $B(E2)$ strength predominantly corresponds to neutron excitations. The ratio of the neutron and proton multipole matrix elements supports such an interpretation.

DOI: 10.1103/PhysRevLett.113.182501 PACS numbers: 21.60.Cs, 23.20.Js, 25.60.Dz, 25.70.De

The study of neutron-rich nuclei with unusually large neutron/proton ratio is challenging the conventional description of the structure of nuclei. Decades of investigation have established that, moving from the β stability towards the drip line, the shell structure undergoes important modifications with the possible disappearance of the usual shell gaps and the emergence of new magic numbers [1,2]. This behavior has been attributed to the dynamic effects of the nucleon-nucleon interaction, to its density dependence, which is linked to the spin-orbit contribution reduction for more diffuse systems, and to the influence of the proton-neutron tensor force [3–6]. Recently, also three-nucleon forces have been invoked to justify the stabilization of the nuclear shells [7]. Unexpected shell modifications have been found all over the nuclear chart, together with the appearance of low-lying intruder states in supposedly semimagic nuclei, giving rise to so-called *islands of inversion*. Examples are the neutron-rich ^{12}Be, ^{32}Mg, and ^{42}Si nuclei which show a large collective behavior [8–10] even if their neutron numbers are well established magic numbers in the stable regions of the nuclear chart ($N = 8, 20$, and 28, respectively).

The Ni isotopic chain ($Z = 28$) covers two doubly closed shells with neutron numbers $N = 28$ and 50, therefore allowing us to test the evolution of the proton gap for neutron rich systems [11]. The $Z = 28$ spherical shell gap lies between the occupied $\pi f_{7/2}$ and the valence $\pi p_{3/2}$, $\pi f_{5/2}$ orbitals. On average, its absolute value amounts to about 5 MeV, large enough to maintain the spherical shape of all Ni isotopes [12]. The filling of the neutron orbitals going towards the heavier isotopes is normally expected to polarize the proton core due to the strong proton-neutron interaction. With an increased number of neutrons, such an effect could be counterbalanced by enhanced configuration mixing due to many body neutron-neutron correlations.

The $B(E2)$ values along a chain of semimagic nuclei provide a sensitive signature of the shell evolution: according to the seniority scheme [13], the $B(E2;0^+ \to 2^+)$ values follow a parabolic trend where the maximum of the parabola corresponds to the middle of the shell and the height depends on the strength of the neutron-induced proton core polarization (for a given proton magic number). $B(E2)$ values smaller than those of the expected parabolic curve indicate the building of a new subshell closure,

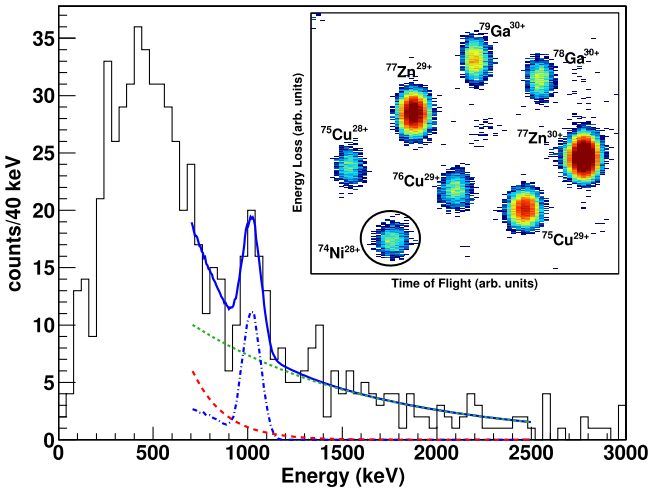

FIG. 1 (color online). Doppler-corrected γ-ray spectrum following Coulomb excitation obtained from the CAESAR detectors when incoming and outgoing particle selections are applied and with the "safe" Coulex impact parameter condition (see text for details). The peak at 1.024 MeV corresponding to the deexcitation of the 2_1^+ state is clearly visible. The spectrum is fitted with the result of a GEANT4 simulation of the response function of the apparatus (dot-dashed blue line) plus two exponential curves (dashed red and green lines) chosen in comparison to background spectra obtained from ^{76}Cu and ^{77}Zn present in the cocktail beam. In the inset, the particle identification plot in the S800 focal plane is reported and the charge state of each isotope is indicated. It shows the energy loss in the focal plane detector versus the time of flight. ^{74}Ni, clearly separated in the plot, was produced with an average rate of 0.7 pps and a purity of 1.5% out of the total.

bigger values suggest an increase of deformation induced by strong core polarization. The comparison of the transition probabilities measured with hadronic and electromagnetic probes can be used to test the nature of the 2^+ state, particularly in the single-closed shell nuclei where such excitations are likely dominated by the valence nucleons.

Transition strengths in the Ni isotopes between $N = 40$ and $N = 50$ have been recently subject of extensive experimental and theoretical investigations (see Refs. [14–16] and references therein). Because of the difficulty of producing such exotic neutron-rich nuclei, experimental $B(E2)$ values determined by means of Coulomb excitation measurements have been limited to ^{70}Ni [11]. In this nucleus, an increase of about a factor 3, as compared to ^{68}Ni, was found and interpreted as evidence of the rapid polarization of the proton core, induced by the filling of the $g_{9/2}$ neutron shell. Furthermore, a recent inelastic proton scattering experiment performed for ^{74}Ni [17] has yielded a large deformation parameter ($\delta^{p,p'}$) that has been interpreted as another sign of enhanced quadrupole collectivity and therefore of the quenching of the $Z = 28$ shell gap for the neutron-rich Ni nuclei.

This Letter reports on the result of an intermediate-energy Coulomb excitation experiment using a radioactive beam of ^{74}Ni, which is presently the heaviest Ni isotope that has been produced with enough intensity to allow the $B(E2)$ measurement. The experiment was performed at the National Superconducting Cyclotron Laboratory (NSCL), Michigan State University. The extracted $B(E2; 0^+ \rightarrow 2^+)$ strength is compared with the results of state-of-the-art large-scale shell-model calculations. To probe the nature of the 2_1^+ excitation, an estimate of the proton-neutron multipole matrix elements ratio (M_n/M_p) has been carried out. This is done assuming the validity of the Bernstein approach described in Ref. [18] and exploiting the combined information of the newly determined transition strength and the one of the inelastic proton scattering experiment [17].

The radioactive ^{74}Ni ion beam was produced via fragmentation as described in Ref. [19]. A stable beam of ^{86}Kr with an intensity of 25 pnA was accelerated by the Coupled Cyclotron Facility to 140 MeV/nucleon and fragmented on a 399 mg/cm^2 thick Be foil at the target position of the A1900 fragment separator [20]. A combination of slits and a 240 mg/cm^2 Al wedge degrader were used to enhance the purity of the fragment of interest in the resulting cocktail beam. A momentum acceptance of $\Delta p/p = 3.0\%$ was used and resulted in a ^{74}Ni beam with an average yield of 0.7 pps and 1.5% purity out of the total. While this acceptance setting provided a sufficient rate of ^{74}Ni for performing the experiment, it added ambiguities in the event-by-event incoming beam identification as discussed later in this section. ^{74}Ni ions impinged on a 642 mg/cm^2 thick ^{197}Au secondary target with a kinetic energy of 95.8 A MeV. The scattered particles were then delivered to the S800 spectrograph [21] and identified at the S800 focal plane using the energy loss versus time-of-flight technique. The mass and charge of the recoiling nuclei were extracted on an event-by-event basis from time-of-flight and energy loss information. The S800 cathode readout drift chamber (CRDC) detectors [22] were used to determine the scattered ions' position and angle in dispersive and nondispersive directions at the focal plane. This information was used to reconstruct the trajectories of the identified particles back to the target position and to determine the impact parameter exploiting the knowledge of the magnetic field in the S800 [21–23]. The reconstruction of the impact parameter is indeed crucial to disentangle the nuclear and the electromagnetic interactions and, therefore, to relate the Coulomb excitation cross section at intermediate energy to the reduced E2 transition probability [24]. The outlined procedure has been validated in a number of successful experiments at NSCL [24–27]. In this way a subset of particle-identified events with the impact parameter larger than 14 fm ("safe" Coulomb cutoff corresponding to the sum of the two nuclear radii plus 2 fm) was selected [26,27]; the corresponding cut on the measured scattering angle was 40 mrad. Gamma rays emitted in

the decay of the Coulomb excited ^{74}Ni nuclei were detected by the CAESAR array composed of 192 CsI(Na) scintillators [28] surrounding the target position. Doppler correction has been performed on an event by event basis using the measured velocity of the recoiling ions and the scattering angle relative to the emitted γ rays. The latter was determined based on the position of the crystal recording the highest energy deposition in a given event. The CAESAR detector was covering approximately 95% of the solid angle with a photo-peak efficiency of about 30% at 1 MeV. Energy calibrations and photo-peak efficiency were determined using standard sources and compared with GEANT4 simulations. Such simulations were used to derive the response function of the array and reproduce the measured efficiencies within 3%. This value was included as a systematic error in the final $B(E2)$ result.

Figure 1 shows the γ-ray spectrum obtained selecting incoming and outgoing ^{74}Ni ions and applying the aforementioned conditions on the scattering angle to satisfy the safe Coulomb excitation requirements. Moreover, only promptly emitted photons were selected through a gate in the γ-ray energy-time correlation. The peak at 1.024 MeV corresponding to the deexcitation of the 2_1^+ state is clearly visible. To determine the number of photons emitted, the spectrum was fitted using the already mentioned simulation. This allows us to take into account the efficiency of the setup, the absorption in the target, and also the Lorentz boost of the emitted γ rays. A double-exponential curve was added to the simulated spectrum in order to account for the beam-induced low-energy bremsstrahlung and the smooth high-energy background. The decay constants of the two exponential curves where estimated from the γ-ray spectra of other nuclei contained in the cocktail beam with larger statistics (namely, ^{76}Cu and ^{77}Zn).

As shown in the inset of Fig. 1, the identification of the scattered ions at the S800 focal plane is straightforward and allows us to clearly select and count ^{74}Ni nuclei. For the incoming cocktail beam tagging, due to the wide momentum acceptance setting of the A1900, a pure isotopic identification is not possible. Despite that, measuring the beam composition in a run without a secondary target and applying the incoming particle selection, it was determined that the only relevant contaminant is ^{76}Cu, which overlaps in the incoming ion selection with the same intensity of ^{74}Ni. The 1.024 MeV γ rays of interest can, therefore, be emitted from the deexcitation of ^{74}Ni produced by the ^{76}Cu $1p$-$1n$ knockout reaction. For this reason, a correction on the experimental data was applied. Using the EPAX code [29], the $1p$-$1n$ knockout cross section was calculated to be 29 mbarn and a 50% population for the 1.024 MeV 2^+ state was assumed. A 50% error is considered for both values. Under these assumptions the ^{76}Cu contribution (number of knockout events with respect to the total number of observed ^{74}Ni ions) turned out to be of the order of 18 out of 3.4×10^5. These ejectiles will yield 9 ± 5 γ rays to be subtracted from the efficiency corrected experimental peak area (where they contribute as 8% of the total). In view of the latter discussion, it is worth noticing that the presence of γ rays coming from the knockout reaction can only cause an over estimation of the Coulomb excitation cross section since this number is subtracted from the total intensity of the γ-ray peak.

The angle-integrated Coulomb excitation cross section to the first 2^+ state was determined as $\sigma_{0^+\to 2^+} = 148^{+50}_{-52}$ mb. Such a value includes the following uncertainties: the errors associated to the fit procedure and to the background modeling, the uncertainties due to the simulated efficiency, the contamination estimate, and the assumption of a fraction of 10% of unobserved feeding from higher lying states. The excitation cross section was then translated into a $B(E2; 0^+ \to 2^+)$ value based on the Coulomb excitation probability calculations performed with the DWEIKO code [30]. A $B(E2; 0^+ \to 2^+) = 642^{+216}_{-226}$ e^2 fm^4 value was obtained. The new experimental result is shown in Fig. 2 together with the measured $B(E2; 0^+ \to 2^+)$ values in the Ni isotopes for $N \geq 40$ [14]. The same figure also includes the results of the following large-scale shell-model calculations.

LNPS: The full pf-shell as proton valence space and the p, $f_{5/2}$, $g_{9/2}$, $d_{5/2}$ orbitals for neutrons, considering ^{48}Ca as an inert core (see Refs. [12,31]). As effective interaction, the two body matrix elements described in Ref. [32] with the monopole changes described in Refs. [12,31] have been used. Effective charges are taken as $(e_p, e_n) = (1.5, 0.5)e$.

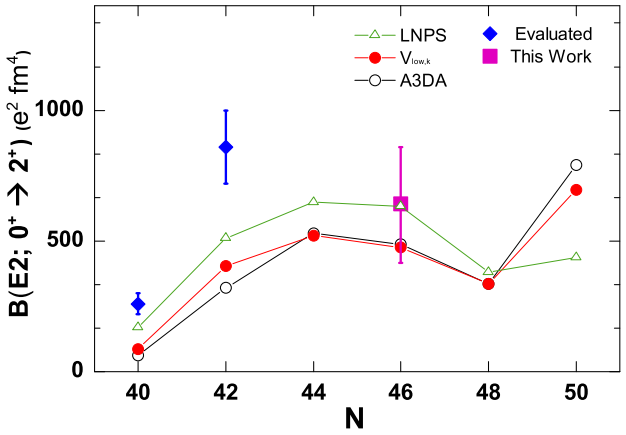

FIG. 2 (color online). Experimental systematic of the $B(E2; 0^+ \to 2^+)$ in the Ni isotopes [14]. The experimental point for ^{74}Ni corresponds to the result of the present Coulomb excitation experiment. From a proton inelastic scattering experiment [17], a model dependent $B(E2; 0^+ \to 2^+)$ value of 1270 ± 380 e^2 fm^4 has also been deduced for ^{74}Ni [14]. The results are compared with the predictions of large-scale shell-model calculations in the $fpgd$ model space and using empirical or derived residual interactions (see text).

$V_{\text{low-}k}$: The $f_{7/2}$, $p_{3/2}$ shells for protons and the $p, f_{5/2}, g_{9/2}, d_{5/2}$ orbitals for neutrons. A two-body effective interaction derived within the framework of perturbation theory (see Refs. [33–35] and references therein) is used starting from the CD-Bonn NN potential renormalized through the $V_{\text{low-}k}$ approach [36] with a cutoff momentum $\Lambda = 2.6$ fm^{-1}. The matrix elements of the effective interaction are calculated using this potential plus a Coulomb force for protons by means of the Q-box folded-diagram expansion as described in Refs. [34,35]. Effective charges are calculated self-consistently [35].

A3DA: A newly enhanced version of the Monte Carlo Shell Model method incorporating the conjugate gradient method and the energy-variance extrapolation taken from Refs. [15,16]. Calculations include the $pfg_{9/2}d_{5/2}$ shells using ^{40}Ca as an inert core and are based on the A3DA residual interaction [37]. Effective charges are taken as $(e_p, e_n) = (1.5, 0.5)e$.

The experimental $B(E2)$ value reported in Fig. 2 for $N = 46$ (present work) disagrees with the model dependent $B(E2)$ value deduced in Ref. [14] from the (p, p') measurement [17]. The experimental uncertainties are large in both experiments as well as in the ^{70}Ni case. We note that our result is comparable to, if not smaller than, the $B(E2)$ measured in the ^{70}Ni case [11]. Despite the large error bars, the value deduced for ^{74}Ni in the Coulomb excitation experiment reported in this Letter is lower than the one deduced from the inelastic proton scattering experiment [14,17]. Moreover, the ^{74}Ni$B(E2)$ value measured in the present work is in good agreement with the results of shell-model calculations using either empirical or microscopic residual interactions. In this context, it should be mentioned that the large $B(E2)$ value of ^{70}Ni has been interpreted as an indication of the strong polarization of the proton core induced by the monopole interaction between the neutron $g_{9/2}$ orbital and the proton $f_{5/2}$ one, see Ref. [11]. The same mechanism would be expected to induce a large transition strength also in ^{74}Ni which is neither found experimentally nor foreseen by the shell model results presented here. It is worth noting that the theoretical $B(E2; 0^+ \to 2^+)$ values at $N = 50$ increase with respect to lighter Ni nuclei, indicating the magicity of the $N = 50$ shell. In fact, as a consequence of the shell closure at $N = 50$, the 2^+ state will not only involve neutron excitations above $N = 50$ but also proton excitations above the $Z = 28$ shell gap in the fp orbits and will therefore have a larger $B(E2)$ value. In order to probe the proton and neutron contributions to the low-lying 2^+ excitation strength of ^{74}Ni, we have used the combined information from Coulomb excitation and from inelastic proton scattering [17]. The proton multipole matrix element M_p is directly related to the reduced electric transition probability since $B(E2; 0^+ \to 2^+) = M_p^2$, whereas, assuming the validity of the Bernstein approach [18], the ratio of the neutron and proton multipole matrix elements is given by

$$\frac{M_n}{M_p} = \frac{N}{Z}\left[\frac{\delta_{p,p'}}{\delta_{\text{em}}} + \frac{Zb_p}{Nb_n}\left(\frac{\delta_{p,p'}}{\delta_{\text{em}}} - 1\right)\right], \quad (1)$$

where $\delta_{p,p'}(\delta_{\text{em}})$ is the deformation length for the hadronic (electromagnetic) probe. A deformation length of $\delta_{p,p'} = 1.04(16)$ fm was measured in Ref. [17]. The corresponding value for δ_{em} extracted from the present $B(E2)$ result is $\delta_{\text{em}} = 0.78 \pm 0.13$ fm ($R = r_0 A^{1/3} = 5.04$ fm) as in Ref. [17]. The interaction strengths of protons with protons (b_p) and with neutrons (b_n) have been chosen to be 0.3 and 0.9, respectively, ([38,39]) including an uncertainty in b_p/b_n of 0.3. This yields $M_n/M_p = 2.4 \pm 0.8$ for the 2^+ state in ^{74}Ni, much larger, even considering the large error, than the value of N/Z expected for a pure isoscalar collective excitation (as in the hydrodynamical model). This ratio, using the LNPS residual interaction, is predicted to be: $M_n/M_p = 1.8$. Large M_n/M_p values have been found in semimagic nuclei with large neutron excess [38,39] and can be qualitatively understood by considering that the valence neutrons are driving the nuclear oscillation and the core polarization is not sufficient enough to restore the isoscalar character of the excitation.

In summary, we have studied the quadrupole collectivity in the neutron-rich ^{74}Ni nucleus ($N = 46$) via intermediate energy Coulomb excitation. The present result provides for the first time a direct measurement of the $B(E2; 0^+ \to 2^+)$ in this nucleus. The new finding is at variance with the value deduced, under the assumption of identical proton and neutron density distribution, from a recent proton inelastic scattering experiment and does not confirm the step rise trend observed for the $B(E2)$ value in ^{70}Ni. The experimental $B(E2)$ value obtained is very well reproduced both by large-scale shell-model calculations using the LNPS effective interaction or the $V_{\text{low-}k}$ approach and the Monte Carlo shell model calculations using the A3DA interaction. The small transition strength observed in ^{74}Ni restores the normal core polarization picture in the neutron rich Ni isotopic chain and suggests that the low-energy $B(E2)$ strength predominantly corresponds to neutron excitations. The large M_n/M_p value estimated based on Ref. [18] supports such an interpretation even if a more detailed analysis will have to be performed with the help, for example, of up-to-date quasiparticle random phase approximation (QRPA) calculations (see Ref. [40]). The extension of the $B(E2)$ and $\delta(p, p')$ systematics in this region will be of high interest to pin down the shell evolution towards the expected doubly magic ^{78}Ni nucleus.

We would like to thank the National Superconducting Cyclotron Laboratory operations staff for stable operation during the experiment. One of the authors, T. M., is also grateful to Centro Universitario Cattolico for financial support. This work was supported by the National Science Foundation under Grants No. PHY-1102511 and No. PHY-0722822 and by the U.S. Department of Energy, Office of Nuclear Physics, under Grant No. DE-FG02-08ER41556.

*Corresponding author.
tommaso.marchi@lnl.infn.it

[1] O. Sorlin and M. G. Porquet, Prog. Part. Nucl. Phys. **61**, 602 (2008).
[2] D. Steppenbeck *et al.*, Nature (London) **502**, 207 (2013).
[3] J. Dobaczewski, I. Hamamoto, W. Nazarewicz, and J. Sheikh, Phys. Rev. Lett. **72**, 981 (1994).
[4] T. Otsuka, T. Suzuki, M. Honma, Y. Utsuno, N. Tsunoda, K. Tsukiyama, and M. Hjorth-Jensen, Phys. Rev. Lett. **104**, 012501 (2010).
[5] T. Otsuka, T. Suzuki, R. Fujimoto, H. Grawe, and Y. Akaishi, Phys. Rev. Lett. **95**, 232502 (2005).
[6] T. Otsuka, M. Honma, and D. Abe, Nucl. Phys. **A788**, 3 (2007).
[7] T. Otsuka, T. Suzuki, J. D. Holt, A. Schwenk, and Y. Akaishi, Phys. Rev. Lett. **105**, 032501 (2010).
[8] H. Iwasaki *et al.*, Phys. Lett. B **491**, 8 (2000).
[9] T. Motobayashi *et al.*, Phys. Lett. B **346**, 9 (1995).
[10] S. Takeuchi *et al.*, Phys. Rev. Lett. **109**, 182501 (2012).
[11] O. Perru *et al.*, Phys. Rev. Lett. **96**, 232501 (2006).
[12] K. Sieja and F. Nowacki, Phys. Rev. C **85**, 051301(R) (2012).
[13] I. Talmi, in *Simple Models of Complex Nuclei, The Shell Model and the Interacting Boson Model* (Harwood Academic, New York, 1993).
[14] B. Pritychenko, J. Choquette, M. Horoi, B. Karamy, and B. Singh, At. Data Nucl. Data Tables **98**, 798 (2012).
[15] N. Shimizu, T. Abe, Y. Tsunoda, Y. Utsuno, T. Yoshida, T. Mizusaki, M. Honma, and T. Otsuka, Prog. Theor. Exp. Phys. **2012**, 1A205 (2012).
[16] Y. Tsunoda, T. Otsuka, N. Shimizu, M. Honma, and Y. Utsuno, Phys. Rev. C **89**, 031301 (2014).
[17] N. Aoi *et al.*, Phys. Lett. B **692**, 302 (2010).
[18] A. M. Bernstein *et al.*, Comments Nucl. Part. Phys. **11**, 203 (1983); A. M. Bernstein, V. R. Brown, and V. A. Madsen, Phys. Lett. **103B**, 255 (1981).
[19] A. Stolz, T. Baumann, T. N. Ginter, D. J. Morrissey, M. Portillo, B. M. Sherrill, M. Steiner, and J. W. Stetson, Nucl. Instrum. Methods Phys. Res., Sect. B **241**, 858 (2005).
[20] D. J. Morrissey, B. M. Sherrill, M. Steiner, A. Stolz, and I. Wiedenhoever, Nucl. Instrum. Methods Phys. Res., Sect. B **204**, 90 (2003).
[21] D. Bazin, J. A. Caggiano, B. M. Sherrill, J. Yurkon, and A. Zeller, Nucl. Instrum. Methods Phys. Res., Sect. B **204**, 629 (2003).
[22] J. Yurkon, D. Bazin, W. Benenson, D. J. Morrissey, B. M. Sherrill, D. Swan, and R. Swanson, Nucl. Instrum. Methods Phys. Res., Sect. A **422**, 291 (1999).
[23] A. Winther and K. Alder, Nucl. Phys. **A319**, 518 (1979).
[24] T. Glasmacher, Annu. Rev. Nucl. Part. Sci. **48**, 1 (1998).
[25] J. M. Cook, T. Glasmacher, and A. Gade, Phys. Rev. C **73**, 024315 (2006).
[26] A. Gade *et al.*, Phys. Rev. C **68**, 014302 (2003).
[27] A. Gade and T. Glasmacher, Prog. Part. Nucl. Phys. **60**, 161 (2008).
[28] D. Weisshaar *et al.*, Nucl. Instrum. Methods Phys. Res., Sect. A **624**, 615 (2010).
[29] K. Summerer and B. Blank, Phys. Rev. C **61**, 034607 (2000).
[30] C. Bertulani, Comput. Phys. Commun. **116**, 345 (1999).
[31] K. Sieja and F. Nowacki, arXiv:1201.0373v1.
[32] S. M. Lenzi, F. Nowacki, A. Poves, and K. Sieja, Phys. Rev. C **82**, 054301 (2010).
[33] L. Coraggio, A. Covello, A. Gargano, N. Itaco, and T. T. S. Kuo, Prog. Part. Nucl. Phys. **62**, 135 (2009).
[34] L. Coraggio, A. Covello, A. Gargano, N. Itaco, and T. T. S. Kuo, Ann. Phys. (Amsterdam) **327**, 2125 (2012).
[35] L. Coraggio, A. Covello, A. Gargano, and N. Itaco, Phys. Rev. C **89**, 024319 (2014).
[36] S. Bogner, T. Kuo, L. Coraggio, A. Covello, and N. Itaco, Phys. Rev. C **65**, 051301 (2002).
[37] M. Honma *et al.* (unpublished).
[38] J. H. Kelley *et al.*, Phys. Rev. C **56**, R1206 (1997).
[39] M. Kennedy, P. Cottle, and K. Kemper, Phys. Rev. C **46**, 1811 (1992).
[40] E. Khan *et al.*, Nucl. Phys. **A694**, 103 (2001).